Fabrication of three-dimensional inter-connective porous ceramics via ceramic green machining and bonding

L. Yin [a,*], H.X. Peng [a], L. Yang [b], B. Su [c]

[a] *Advanced Composites Centre for Innovation and Science (ACCIS), Department of Aerospace Engineering, Faculty of Engineering, University of Bristol, Queens Building, University Walk, Bristol BS8 1TR, UK*
[b] *School of Chemistry, Faculty of Science, University of Bristol, Cantock's Close, Bristol BS8 1TS, UK*
[c] *Department of Oral and Dental Science, Faculty of Medicine and Dentistry, University of Bristol, Lower Maudlin Street, Bristol BS1 2LY, UK*

Abstract

A novel method is demonstrated to fabricate three-dimensional inter-connective porous ceramics with engineered structures. The method is based on machining and bonding of ceramic green sheets. The ceramic green sheets were processed via a viscous polymer processing (VPP) route using thermoplastic (polyvinyl butyral) as a binder, which showed good machinability and surface finishing quality. The experimental results also revealed that an appropriate solvent and adequate applied pressure were critical to ensure good interfacial bonding between green ceramic sheets and subsequent integrity of the sintered three-dimensional inter-connective ceramic bodies. The architectures and microstructures of fabricated ceramic bodies can be readily controlled by the characteristics of the green body and the computer numerically controlled machining conditions.
© 2007 Elsevier Ltd. All rights reserved.

Keywords: Al$_2$O$_3$; Joining; Ceramic green machining; Porosity; Microstructure

1. Introduction

Porous ceramics have been widely used in various technological applications, such as lightweight and impact-resistant materials, thermal insulation and high temperature combustion burners, corrosion-resistant filters and bone tissue engineering scaffolds.[1] Among the processing routes developed for the production of porous ceramics for specific applications, conventional replication, sacrificial template and direct foaming methods have been extensively researched and reviewed.[2,3] The microstructural features that determined the mechanical and functional properties of porous ceramic, e.g., open or closed porosity, pore size distribution and pore morphology, are highly influenced by the processing methods and conditions used for the production of the porous materials.[4–6]

Due to limited control over microstructural features such as shape, dimension and inter-connectivity in the conventional methods mentioned above, a number of advanced approaches have been developed to fabricate ceramic products with well-defined 3D architectures and microstructures. Solid freeform fabrication (SFF) techniques such as stereolithography (SLA), selective laser sintering (SLS), three-dimensional printing (3DP), direct ink-jet printing, robocasting, fused deposition modeling (FDM) and micro-pen writing provide powerful routes to produce complex 3D structures with controlled architectures.[7,8] Although the SFF techniques have achieved more success in polymers and metals, the quality of ceramic components produced by the SFF techniques is less satisfactory. Staircase effect caused from the layer-by-layer process is a typical feature in the SFF techniques through powder-, droplet- or filament-based approaches. Though the quality of finished surfaces could be improved by reducing layer thickness or by post-processing such as grinding or polishing, they are often at the expense of massive increase of production time and cost. The SFF techniques have been widely reported to fabricate 3D ceramic lattice structures primarily for tissue engineering scaffold applications because the feature size and resolution of the current SFF technology can meet the requirements for tissue engineering scaffolds. But the mechanical properties of the ceramic scaffolds thus, produced are far from optimal. An

---

* Corresponding author. Tel.: +44 117 3317917; fax: +44 117 9272771.
E-mail address: lei.yin@bristol.ac.uk (L. Yin).

alternative route to fabricate 3D porous ceramics with defined architectures is via an indirect SFF technique, i.e. a negative polymer template is first built up by using the SFF techniques such as stereolithography, ceramic slurry is then infiltrated into the polymer template. After debinding and sintering, a positive ceramic structure with controlled pore units could be produced.[9]

With the advances in computer numerically controlled (CNC) machining technique and ceramic green body forming technique, green ceramic machining is being developed as an alternative for rapid-prototyping of ceramics.[10] Compared with the SFF techniques, green ceramic machining represents a top-down approach for the rapid fabrication of ceramic bodies. It provides an option to fabricate the ceramic components at relatively lower costs, higher production speed and with less restriction in specimen dimensions.[11,12]

In the green ceramic machining process, the green body should have sufficient strength to withstand the tooling force and exhibit good machinability during machining. Therefore, the choice of binder and dispersed system is critical to achieve high ceramic solid loading, uniformly distributed particles in green body, strong interfacial bonding between ceramic particles and adequate strength of green body.[13] In addition, the high solid loading in green body results in less sintering shrinkage.

Previous works demonstrated that the surface finish and dimensional accuracy could be significantly improved if appropriate ceramic green body and machining condition were selected.[10] A recent study showed that the ceramic green body with a thermoplastic binder had good machinability.[14] Unlike the thermosetting polymers which, once formed and cured, cannot be remelted and remolded. The thermoplastic polymers can be either reshaped by reheating or bonded together by applying a solvent to diffuse into the polymers. For example, the machined green ceramics can be assembled by thermo-compression, in which the green tapes are joined by applying an uniaxial high pressure at a temperature above the glass transition temperature (T_g) of binders.[15] However, the fine structures or patterns in green body cannot easily be retained at such elevated temperature and high pressure.[16] Therefore, low temperature and low pressure lamination techniques have been investigated. It has been demonstrated that the green tape can be joined together by applying either adhesive tapes or polymer binder solutions under low temperature and low pressure conditions. After debinding and sintering, seamless ceramic body can be produced.[17,18]

Recently a CNC machining/coating method was reported to fabricate 3D ceramic porous structures.[19] In this method, a graphite inter-connective 3D architecture was built by biaxial pore channels, which was then used as a template to fabricating porous ceramics by ceramic slurry dip-coating and sintering. In the present work, we propose to use direct CNC machining and bonding of green ceramics to fabricate 3D inter-connective ceramics. The unique porous ceramics with controlled open-pore microstructures and 3D architectures have potentials in many applications, such as reinforcement preform for the fabrication of bi-continuous or interpenetrating phase composites (IPCs) and bone tissue engineering scaffolds.[20,21]
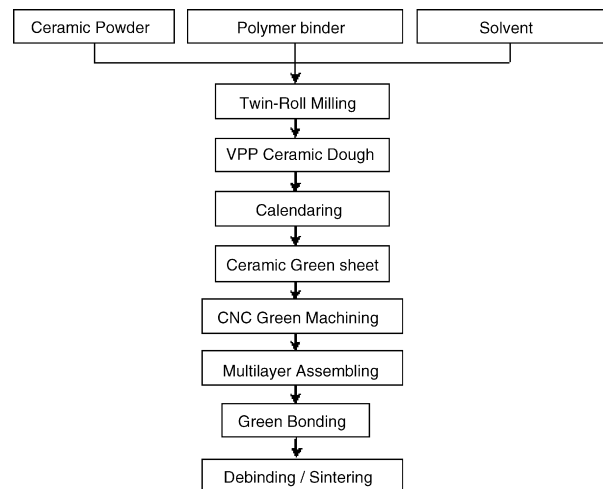

Fig. 1. Flow chart for the fabrication of inter-connective porous ceramic by direct green machining and bonding method.

2. Experimental details

The flow chart for the fabrication of 3D inter-connective porous ceramics with defined architecture is shown in Fig. 1. Essentially, alumina powder ($D_{50} = 0.3\,\mu$m) was premixed with polyvinyl butyral (PVB) binder and cyclohexanone was chosen as a solvent. After mixing and twin-roll milling, the VPP ceramic dough was obtained. After degassing under a press for 10 h, the VPP ceramic dough was calendared into sheets with desired thickness. The final ceramic green sheets were obtained by heating the VPP ceramic sheets in oven at 115 °C for 14 h. The thickness of ceramic green sheets used in this study varied from 0.7 mm to 1.5 mm. Green machining was performed on a Roland bench-top CNC milling machine (MDX 650, Roland DG Ltd., Japan). According to previous study,[10] end mill diamond coated carbide tools were selected for CNC machining of the green ceramics. A vacuum table was used to hold the samples during machining. The ceramic green sheet with 0.8 mm thickness was machined into 20 m × 20 m square units, which had periodic channels on both sides but intersected each other in orthogonal direction. The gap and channel size were in range from 0.8 to 1.5 mm and 1.0 to 1.5 mm, respectively.

The machined green sheets were put on a filter paper which was saturated with 1-butanol solvent (99.4%, Sigma Aldrich) for 15, 30, 60, 90 and 120 s, respectively. Three-dimensional green body was assembled manually by laminating the solvent-coated green ceramic sheets together under a pressure varied from 0.2 to 3 MPa for 12 h. For mass production with precision assembly, automation using an assembly jig could be carried out to control the dimensional accuracy. Finally, porous ceramics were fabricated by binder burn-out at a heating rate of 1 °C/min to 550 °C for 2 h followed by sintering at a heating rate of 10 °C/min to 1500 °C for 2 h.

The flexural strength of green sheet was measured in three-point bending mode with sample dimension of 0.8 mm × 2 mm × 30 mm. Test was performed on a twin column testing machine (Lloyd Instruments Ltd., LR5K) with a span of 20 mm and a crosshead speed of 0.5 mm/min. The microstruc-

tures of the green sheet and ceramic body were characterized by using scanning electron microscope (SEM JEOL JSM5600LV). Surface characterization was carried out by using a non-contact profilometer (Scantron Proscan 2000, Scantron Industrial Products Ltd., U.K.). Two different machining modes including roughing and finishing were investigated. The machined surfaces were compared with the original surfaces of green sheets.

3. Results and discussion

3.1. Machinability of green ceramic sheets

Machinability of ceramic green body depends on the machining condition and the mechanical properties of green body.[13,14] Previous studies have revealed that among different tool materials, the use of diamond coated tools achieved the best surface finishing.[10] After comparing different cutting parameters, such as spinning speed, speed along x–y and z direction, cutting-in amount and path interval distance, the optimized cutting parameters were found to be 12000 rpm with maximum x–y speed of 8 mm/s in the present work. Other parameters, like cutting-in amount and path interval distance are varied in different machining modes.

A scanning electron microscope (SEM) image of the ceramic green is shown in Fig. 2. It can be seen that the alumina particles were uniformly distributed and closely packed in the green body without severe surface defects, such as crack, void and particles pull-out. The flexural strength of the green sheet was measured to be 106.02 MPa. This indicates that the green sheets process sufficient strength to be machined, which the details will be discussed later.

Fig. 3(a) shows a straight and square sharp groove in as-machined green sheet with a good accuracy in dimension control. A sharp edge was well maintained during machining without any chips and cracks being observed. The effectiveness of swarf removal is one of the important factors that affect the surface finish quality of a machined product. Although the
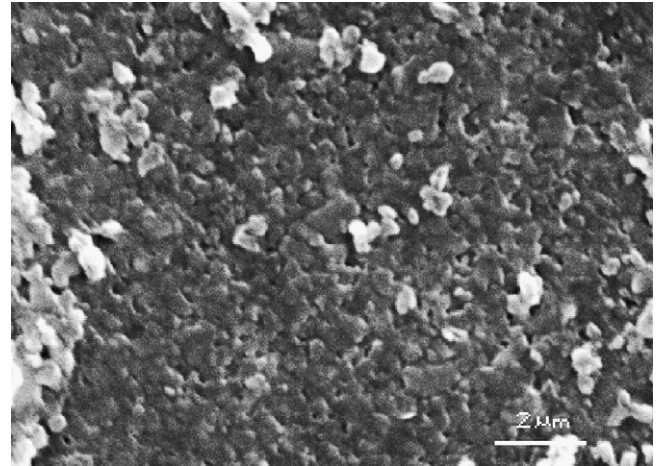

Fig. 2. SEM micrograph of the original surface of ceramic green body.

forming type of swarf can be broadly categorized into either obstruction-type or groove-type, the basic forming action is the same.[22] The swarf is constrained to move in a circular path and the free end of the swarf impinges on the flank face of the cutting tool or tool-holder. At this stage, the free end of the swarf anchors itself to the contact point and subsequent swarf production results in an increase in the radius of curvature of the formed swarf. Under optimal conditions, as the swarf size and the radius increase, a stage is reached when the stress in the swarf is so high that it breaks. Fig. 3(b) shows the morphology of swarfs formed during machining. The half circular shape indicates that the swarf generated in this work is a typical effectively broken form.[22] It was also observed that discontinuous swarfs were consistently formed and removed from the cutting zone easily during the machining process.

The high resolution SEM image of the machined surface of green ceramic body is given in Fig. 4. It is clear that negligible tearing and pull-out of particles were observed on the machined surface, indicating a good quality of surface finish was obtained. It is found that during the machining of thermoplastic poly-
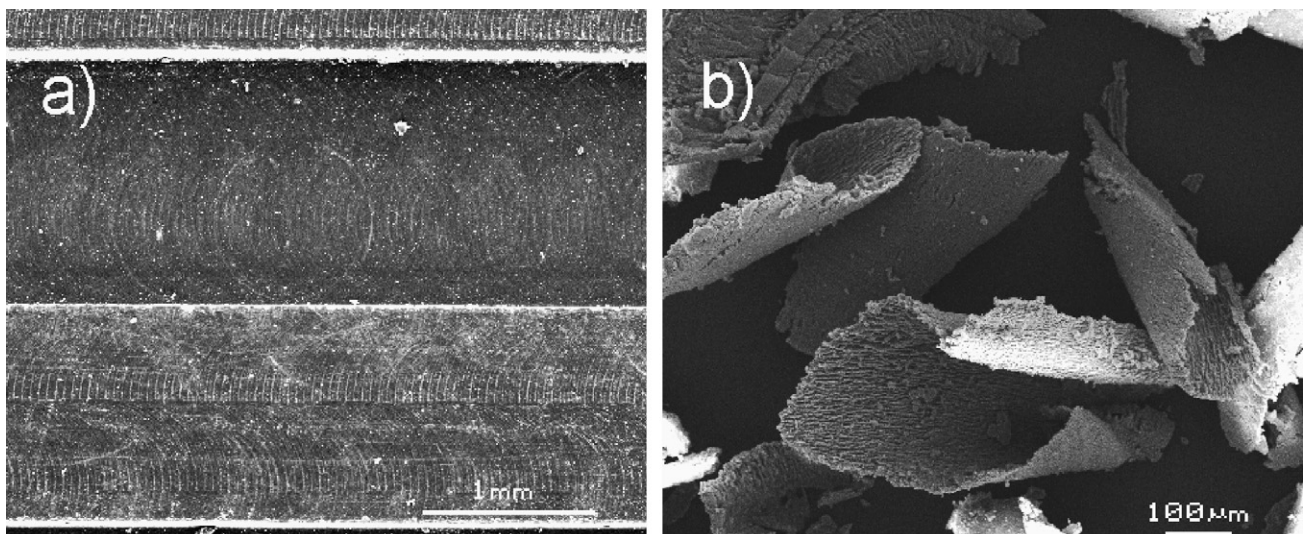

Fig. 3. (a) Machined ceramic green body with square channel and (b) morphology of collected swarfs during machining.
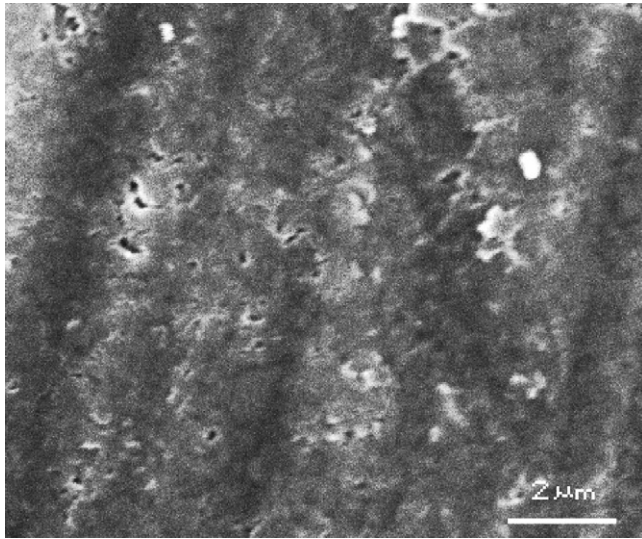
Fig. 4. SEM micrograph of the surface of as-machined ceramic green sheet.

Table 1
Characteristics of ceramic green body

Density (g/cm^3)	2.58
Flexural strength (MPa)	106.02 ± 5.68
Surface roughness (μm)	
Original surface	17.96
Roughing surface	2.78
Finishing surface	2.60

melting. It is therefore suggested that, in order to minimize the surface roughness, for instance, the machining conditions must be selected in such a way that the material removal deformation falls in the regime without visco-plastic scaling/tearing and brittle cracking.

The results of surface roughness measurements (see Table 1) indicated that the surface of green body became smoother after machining. Although similar surface roughness was observed for both roughing and finishing machining modes, the regular marks along the path of tool movement, which can be seen from the 3D surface profile shown in Fig. 5, are varied in different machining modes. The distance between each mark under finishing mode is smaller than that under roughing mode. The difference was due to the smaller path interval in the finishing mode. The particle size and tool size may also affect the quality of surface finishing, especially when the feature size is close

mer, the material can be removed in a ductile or brittle manner, depending on the characteristics of the polymer related to its T_g.[23] If the local temperature is below T_g, the material tends to be removed in a brittle way. Otherwise, the material tends to be removed in a ductile manner with extensive deformation or
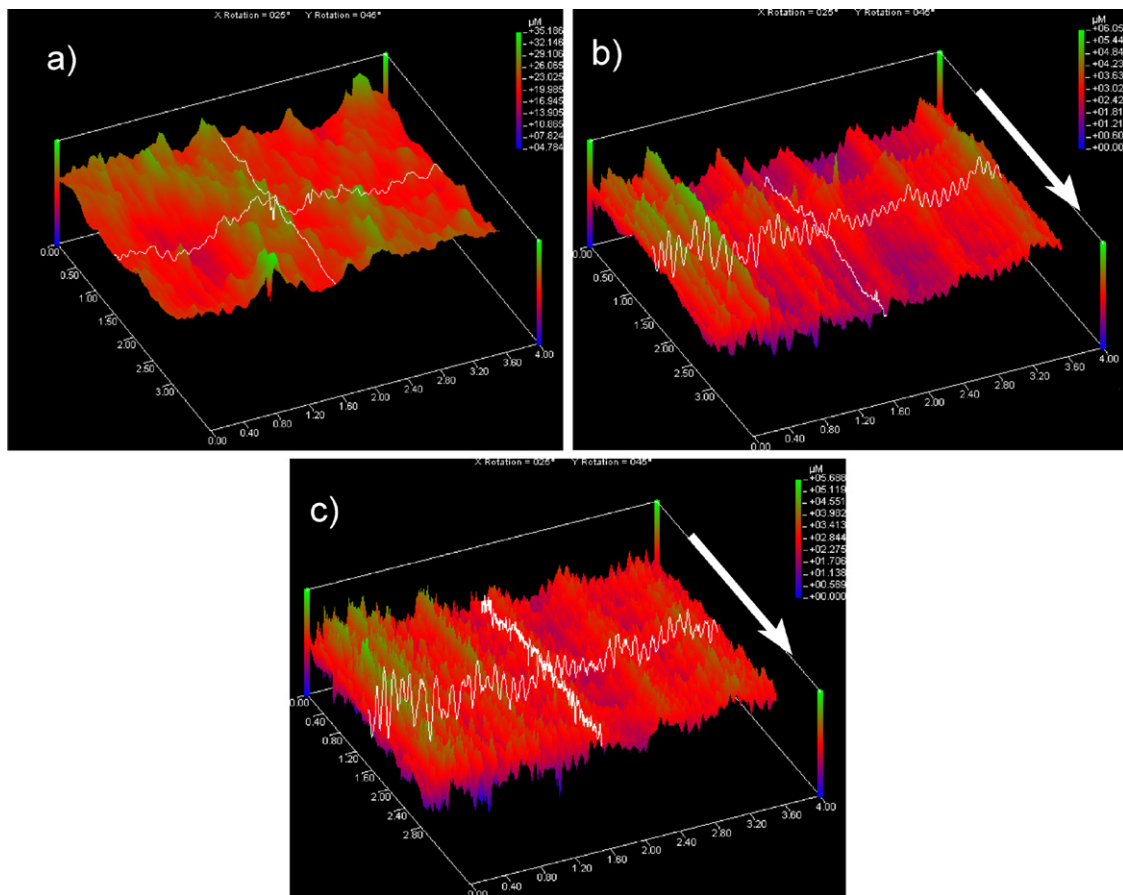

Fig. 5. 3D surface roughness profiles of (a) original green body, (b) machined green body under roughing mode and (c) machined green body under finishing mode (arrows indicating the tool moving direction).
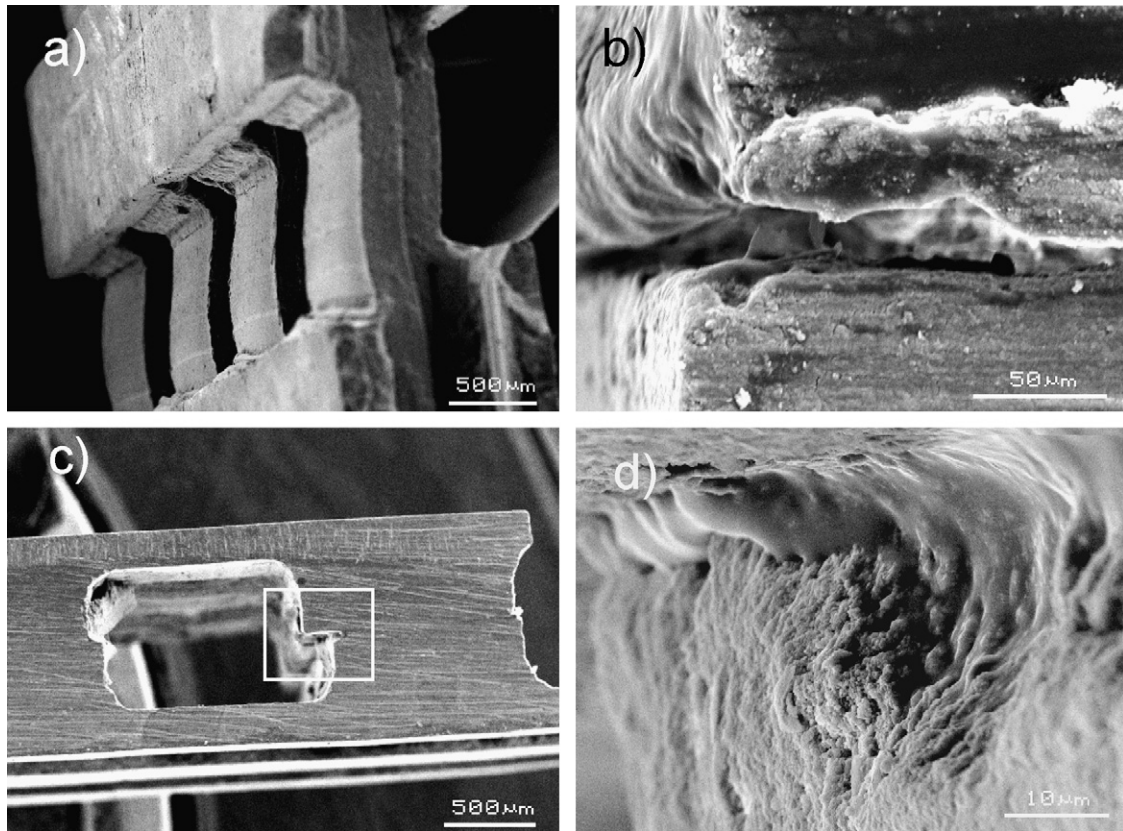
Fig. 6. SEM micrographs of selected green bodies after the green bonding process showing (a) deformation caused by too much solvent applied during bonding, (b) delaminated interface under bonding pressure of 0.05 MPa, (c) seamless bonding under pressure of 0.25 MPa and (d) high magnification of the framed region in (c).

to the raw materials size and tool size. It is clear that the surface feature of machined green body is strongly related to the machining conditions.

3.2. Green bonding of ceramic sheets

PVB binder shows good solubility in alcoholic solvent. The 1-butanol was chosen because of its relatively high boiling point of 117.7 °C and low evaporative rate, so that the bonded interface between machined green sheets has enough time to diffuse. After comparing green bodies with the varied soaking time on solvent saturated filter paper, it was found the optimized time was between 45 and 60 s for a solvent film to form on green sheet which can then be bonded. If the amount of solvent on interface is insufficient, inferior diffusion and bonding occurs between layers. On the contrary, too much solvent can cause severe decrease in bonding strength between layers. In addition, deformation may occur under applied pressure during bonding process, which will affect the accuracy of the shape and dimension of the resulting 3D green body and the subsequent sintered ceramic body (see Fig. 6(a)).

In order to facilitate the bonding between laminated green ceramic sheets, pressure was applied in perpendicular to the bonding interface. The effect of pressure on the bonding was examined by comparing samples bonded under different pressures. Experimental results showed that delamination occurred if the applied pressure was below 0.05 MPa (see Fig. 6(b)).

When pressure was increased to 0.15 MPa, the interface is visible near the edge of ceramic sheets. The optimized pressure was found to be 0.25 MPa where green ceramic sheets were fully diffused and bonded together. As illustrated in Fig. 6(c), the machined structures are well retained and interface can be hardly seen. Nevertheless the machined green structure could be deformed when the applied pressure was beyond the optimal value. Fig. 6(d) is a high magnification image of the bonding area (the framed region in Fig. 6(c)). It is evident that good bonding has been achieved. Therefore, it is practically feasible

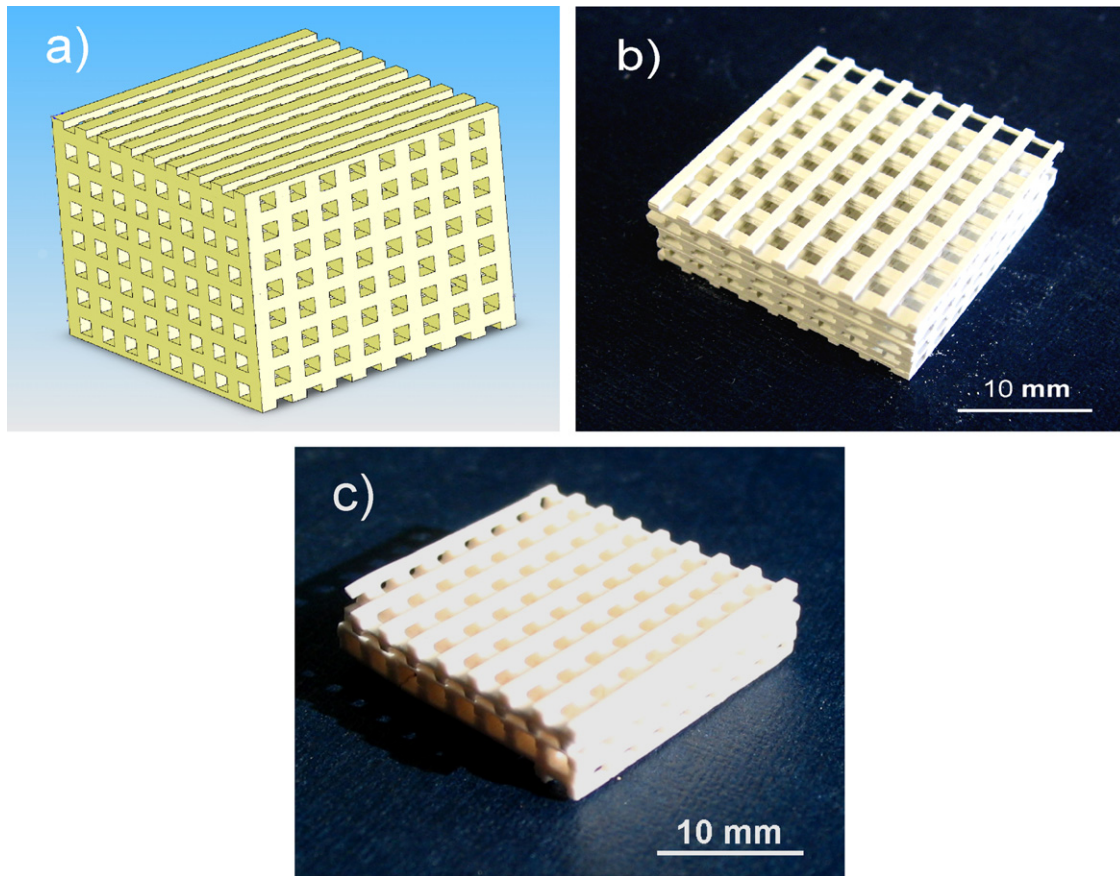Fig. 7. SEM micrograph of cross-section of sintered ceramic sample showing good bonding between layers.

Fig. 8. Demonstration of a 3D inter-connective ceramic structure (a) computer-aided design (CAD) structure, (b) machined and assembled ceramic green structure and (c) sintered inter-connective ceramic structure.

to obtain a seamless bonding between individual green ceramic sheets using a low pressure green bonding technique.

3.3. Debinding and sintering

After debinding and sintering, the 3D ceramic sample had ∼15% linear shrinkage, but still showed good shape retention. No cracks or deformation can be seen at bonded region (Fig. 7). It was found that bonding played an important role in the final quality of 3D ceramic structures. Once the green sheets are well bonded, then the final sintered ceramic structure is most likely to be integrated without delamination and cracking.

Fig. 8 illustrated the feasibility to fabricate an inter-connective porous ceramic structure using the green machining and bonding method. The dimension of the demonstrated 3D green body is 20 mm × 20 mm × 8 mm. The width of the gap and channel are both 1 mm (Fig. 8(b)). After sintering, the resulted porous ceramic body is about 17 mm × 17 mm × 6.8 mm. Because of the high green strength and toughness of green ceramic sheets prepared from the VPP technique, it is anticipated that the dimension of the green machined ceramic components can be readily extended to much larger size than those produced using direct ink writing or printing, where weak ceramic green bodies may collapse when building up too many layers. While the feature size of green machined ceramics is mainly determined by the cutting tool size and the tolerance of the

CNC machine, it is possible to produce 3D inter-connective ceramics with pore size of ∼500 μm. These 3D porous ceramics with well-defined unit cell size and inter-connectivity will find applications in many areas, such as bioceramic scaffolds for bone tissue engineering or ceramic preforms for novel inter-penetrating composite materials and ceramic micro-reactors and micro-fuel cells for micro-electromechanical systems (MEMS).

4. Conclusions

3D inter-connective porous ceramics with predefined structure have been fabricated using a combined green machining and bonding technique. The ceramic green sheets made from the VPP method possessed high green strength and good machinability. The machined dual channel green sheet had good surface finishing quality. The experimental results also showed that the choice of solvent and applied pressure is critical during the green bonding process in order to retain the integration and dimension of subsequently sintered ceramics. The fine features and microstructures can be controlled by the dimension of cutting tools and tolerance of CNC machine, as well as the characteristics of the green ceramics and machining conditions. The novel combination of ceramic green machining and bonding method can be potentially developed as an alternative rapid-prototyping process for the production of complex shaped ceramic compo-

nents. The 3D inter-connective porous ceramics demonstrated in this work can be potentially used as reinforcement for interpenetrating composites and as scaffolds for bone tissue engineering applications. More complex cellular structures of ceramics could potentially be fabricated using the methodology described in this work for a wider range of applications.

Acknowledgements

References

1. Lorna, J. G. and Michael, F. A., *Cellular Solids: Structure and Properties* (*2nd ed.*). Cambridge University Press, Cambridge, 1997.

2. Studart, A. R., Tonzenbach, U. T., Tervoort, E. and Gauckler, L. J., Processing routes to macroporous ceramics: a review. *J. Am. Ceram. Soc.*, 2006, **89**, 1771–1789.

3. Colombo, P., Conventional and novel processing methods for cellular ceramics. *Phil. Trans. R. Soc. A*, 2006, **364**, 109–124.

4. Innocentini, M. D. M., Sepulveda, P., Salvini, V. R. and Pandolfelli, V. C., Permeability and structure of cellular ceramics: a comparison between two preparation techniques. *J. Am. Ceram. Soc.*, 1998, **81**, 3349–3352.

5. Lee, B. T., Kang, I. C., Cho, S. H. and Song, H. Y., Fabrication of a continuously oriented porous Al2O3 body and its in vitro study. *J. Am. Ceram. Soc.*, 2005, **88**, 2262–2266.

6. Dhara, S. and Bhargava, P., Influence of slurry characteristics on porosity and mechanical properties of alumina foams. *Int. J. Appl. Ceram. Technol.*, 2006, **3**, 382–392.

7. Tay, B. Y., Evans, J. R. G. and Edirisinghe, M. J., Solid freeform fabrication of ceramics. *Int. Mater. Rev.*, 2003, **48**, 341–370.

8. Lewis, J. A., Smay, J. E., Stuecker, J. and Cesarano III, J., Direct ink writing of three-dimensional ceramic structures. *J. Am. Ceram. Soc.*, 2006, **89**, 3599–3609.

9. Woesz, A., Rumpler, M., Stampfl, J., Varga, F., Fratzl-Zelman, N., Roschger, P., Klaushofer, K. and Fratzl, P., Towards bone replacement materials from calcium phosphates via rapid prototyping and ceramic gelcasting. *Mater. Sci. Eng. C: Biomimetic Upermol. Syst.*, 2005, **25**(2), 181–186.

10. Dhara, S. and Su, B., Green machining to net shape alumina ceramics prepared using different processing routes. *Int. J. Appl. Ceram. Technol.*, 2005, **2**, 262–270.

11. Maier, H. R. and Michaeli, N., Green machining of alumina. *Key Eng. Mater.*, 1997, **132–136**, 436–439.

12. Lindqvist, K. and Carlstrőm, E., Green machining of alumina formed by CIP, starch consolidation and latex slip casting. *Key Eng. Mater.*, 2002, **206–213**, 301–304.

13. Kaşgozǒ, A., őzbaş, Z., Kaşgőz, H. and Aydin, I., Effects of monomer composition on the mechanical and machinability properties of gel-cast alumina green compacts. *J. Eur. Ceram. Soc.*, 2005, **25**, 3547–3552.

14. Koh, Y. H. and Halloran, J. W., Green machining of a thermoplastic ceramic-ethylene ethyl acrylate/isobutyl methacrylate compound. *J. Am. Ceram. Soc.*, 2004, **87**, 1575–1577.

15. Rosaura, H. S. and Wilkinson, D. S., Strength of tape cast and laminated ceramics. *J. Am. Ceram. Soc.*, 1995, **78**, 1580–1584.

16. Roosen, A., Low-temperature/low-pressure lamination of green ceramic tapes. *Adv. Eng. Mater.*, 2000, **2**, 374–376.

17. Suppakarn, N., Ishida, H. and Cawley, J. D., Roles of poly(propylene glycol) during solvent-based lamination of ceramic green tapes. *J. Am. Ceram. Soc.*, 2001, **84**, 289–294.

18. Roosen, A., New lamination technique to join ceramic green tapes for the manufacturing of multilayer devices. *J. Eur. Ceram. Soc.*, 2001, **21**, 1993–1996.

19. Jun, I. K., Koh, Y. H., Song, J. H. and Kim, H. E., Fabrication and characterization of dual-channeled zirconia ceramic scaffold. *J. Am. Ceram. Soc.*, 2005, **89**, 2021–2026.

20. Peng, H. X., Fan, Z. and Evans, J. R. G., Bi-continuous metal matrix composites. *Mater. Sci. Eng. A*, 2001, **303**, 37–45.

21. Chen, Q. Z., Boccaccini, A. R., Zhang, H. B., Wang, D. Z. and Edirisinghe, M. J., Improved mechanical reliability of bone tissue engineering scaffolds by electrospraying. *J. Am. Ceram. Soc.*, 2006, **89**, 1534–1539.

22. Mills, B. and Redford, A. H., *Machinablility of Engineering Materials*. Applied Science, London, 1983, pp. 21–31.

23. Xiao, K. Q. and Zhang, L. C., The role of viscous deformation in the machining of polymers. *Int. J. Mech. Sci.*, 2002, **44**, 2317–2336.